Received: 10 May 2022 | Revised: 30 November 2022 | Accepted: 3 December 2022

DOI: 10.1002/jnr.25154

MINIREVIEW

JOURNAL OF Neuroscience Research

Review of individualized current flow modeling studies for transcranial electrical stimulation

Alexander Hunold[1] | Jens Haueisen[1] | Frauke Nees[2] | Vera Moliadze[2]

[1]Institute of Biomedical Engineering and Informatics, TU Ilmenau, Ilmenau, Germany

[2]Institute of Medical Psychology and Medical Sociology, University Medical Center Schleswig Holstein, Kiel University, Kiel, Germany

Correspondence
Alexander Hunold, Institute of Biomedical Engineering and Informatics, TU Ilmenau, Gustav-Kichhoff-Str. 2, 98693 Ilmenau, Germany.
Email: alexander.hunold@tu-ilmenau.de

Funding information
Deutsche Forschungsgemeinschaft, Grant/Award Number: SFB1158/B03; European Commission; Thüringer Aufbaubank; Thüringer Ministerium für Wirtschaft, Wissenschaft und Digitale Gesellschaft; Free State of Thuringia, Grant/Award Number: 2021 FE 9098, 2018 IZN 004 and 2017 VF 0035

Abstract

There is substantial intersubject variability of behavioral and neurophysiological responses to transcranial electrical stimulation (tES), which represents one of the most important limitations of tES. Many tES protocols utilize a fixed experimental parameter set disregarding individual anatomical and physiological properties. This one-size-fits-all approach might be one reason for the observed interindividual response variability. Simulation of current flow applying head models based on available anatomical data can help to individualize stimulation parameters and contribute to the understanding of the causes of this response variability. Current flow modeling can be used to retrospectively investigate the characteristics of tES effectivity. Previous studies examined, for example, the impact of skull defects and lesions on the modulation of current flow and demonstrated effective stimulation intensities in different age groups. Furthermore, uncertainty analysis of electrical conductivities in current flow modeling indicated the most influential tissue compartments. Current flow modeling, when used in prospective study planning, can potentially guide stimulation configurations resulting in individually effective tES. Specifically, current flow modeling using individual or matched head models can be employed by clinicians and scientists to, for example, plan dosage in tES protocols for individuals or groups of participants. We review studies that show a relationship between the presence of behavioral/neurophysiological responses and features derived from individualized current flow models. We highlight the potential benefits of individualized current flow modeling.

KEYWORDS
age, current flow simulation, forward modeling, precision medicine, transcranial electrical stimulation (tES)

Frauke Nees and Vera Moliadze shared authorship.

Edited by Cristina Antonella Ghiani and Elizabeth Johnson. Reviewed by Jose Gomez-Tames, Alessandra Vergallito, and Daria Antonenko.

1 | INTRODUCTION

Noninvasive transcranial electrical stimulation (tES) includes direct current (tDCS), alternating current (tACS), and random noise stimulation (tRNS) (Paulus, 2011). The neuromodulatory effects of these techniques have been used in neuroscience to investigate brain function (Vosskuhl et al., 2018) and in clinical research to derive new therapies (Fregni et al., 2021; Lefaucheur et al., 2017). During the last two decades, studies provided essential insights into the mechanisms of action of tES (Fertonani & Miniussi, 2017; Reed & Cohen Kadosh, 2018). However, there is substantial variability in the responses to tES across subjects and within subjects across multiple stimulation sessions, which represents one of the most important limitations of tES (Fertonani & Miniussi, 2017; Guerra et al., 2020; Horvath et al., 2014; Krause & Kadosh, 2014; Li et al., 2015; Medina & Cason, 2017; Vergallito et al., 2022).

Experimentally, often a one-size-fits-all approach is used, in which a generic stimulation protocol of a particular electrode setup and stimulation intensity is applied to all participants. This neglects interindividual anatomical and physiological differences.

For example, studies have shown that with an identical montage and setup the effects of tDCS on cognitive functions can vary (Hsu et al., 2016; Splittgerber et al., 2020; Tseng et al., 2012). Clinical studies showed that the same stimulation protocols with the same stimulation parameters may not be optimal in different patients (Cappon et al., 2016). Due to the individual anatomy of the head, the same stimulation setup and parameters will yield different electric fields (Datta et al., 2012; Kim et al., 2014) in the targeted and nontargeted brain regions. Consequently, the generic one-size-fits-all approach might be one of the reasons for the substantial outcome variability (Karabanov et al., 2016; Krause & Kadosh, 2014; Li et al., 2015).

While the number of tES studies has grown significantly, the reproducibility of these studies remains a challenge. A survey found that with tDCS only 45%–50% of researchers were able to routinely replicate published effects (Héroux et al., 2017). Although less research was published on tACS, similar reproducibility problems have been reported (Brauer et al., 2018; Coldea et al., 2021; Jones et al., 2019; Veniero et al., 2017).

One possible reason for null effects or failed replications could be the differences in anatomy, which affect the amount of current entering the brain and the distribution of current in the brain. For example, the magnitudes of neurophysiological modulations induced by tDCS were identified to be significantly associated with individual simulation-based electric field strengths within the targeted left precentral gyrus (Antonenko et al., 2019). However, about 2/3 of the studies included in a recent review summarizing the effects of single-session tDCS on reactive response inhibition in the stop-signal task performance incorporated no current flow modeling (Friehs et al., 2021).

Current flow modeling describes the quantification of the electric field and the electric current density throughout the entire head. Typically, the quasi-stationary approximation of Maxwell's equations is applied in tES current flow modeling. Under this assumption, the electric field and the current density are considered to be linearly linked via the conductivity values of the modeled tissues. In this review, we focus on interpretations of the electric field as this measure is more frequently used in the considered literature. However, that does not limit the generality, since the considered linear relationship allows a transfer of the interpretations to the current density.

Significance

Transcranial electrical stimulation (tES) is a promising methodology for interventional neurophysiology used in both scientific and therapeutic applications. Many tES protocols apply fixed parameters to all participants or patients contributing to outcome variability. Here we review studies using individualized modeling to derive adapted stimulation configurations leading to more robust stimulation effects.

tES applications intend to modulate the activity in one or more specific, target brain regions. The electric field is a major determinant for the initiation of the physiological and thus the behavioral stimulation effect (Liu et al., 2018; Peterchev et al., 2012). Therefore, the stimulation setup should be determined with respect to the generated field in the target areas (Bergmann & Hartwigsen, 2020; Evans et al., 2020). At the same time, the electric field possibly also modulates activity in other, nontarget brain regions (Gomez-Tames et al., 2020). Moreover, target and nontarget regions interact through their neuronal networks. Consequently, the induced electric field should be analyzed in both the target and the nontarget regions. Both the individual anatomy and the neuronal network structure have considerable intersubject variability which affect tES outcome.

The orientation of the target[1] has an important role as the electric field exerts its effect along the field orientation but has a negligible effect for vectors orthogonal to the field orientation (Liu et al., 2018). Cortical pyramidal cells show a systematic alignment perpendicular to the cortical surface. Assemblies of pyramidal cells can be modeled as an equivalent dipole and, at the same time, as a neural mass in a neural mass model, see Figure 1.

Based on the estimation of electric fields in the brain, the electrode placement and the applied current strength can be inversely defined to optimally target a specified brain region which was modeled as a dipole in the brain. Modeling current flow, therefore, provides the basis for tES optimization to provide the stimulation to the target brain regions (Dmochowski et al., 2017; Gomez-Tames et al., 2019; Guler et al., 2016; Ruffini et al., 2014; Wagner et al., 2016). Optimization strategies have different goals that are expressed through goal functions and constraints. For example, one might want to maximize the field strength at a set of target regions with specific target orientations. However, due to the restrictions inherent to tES, all optimization results essentially represent a compromise between a wished stimulation at target

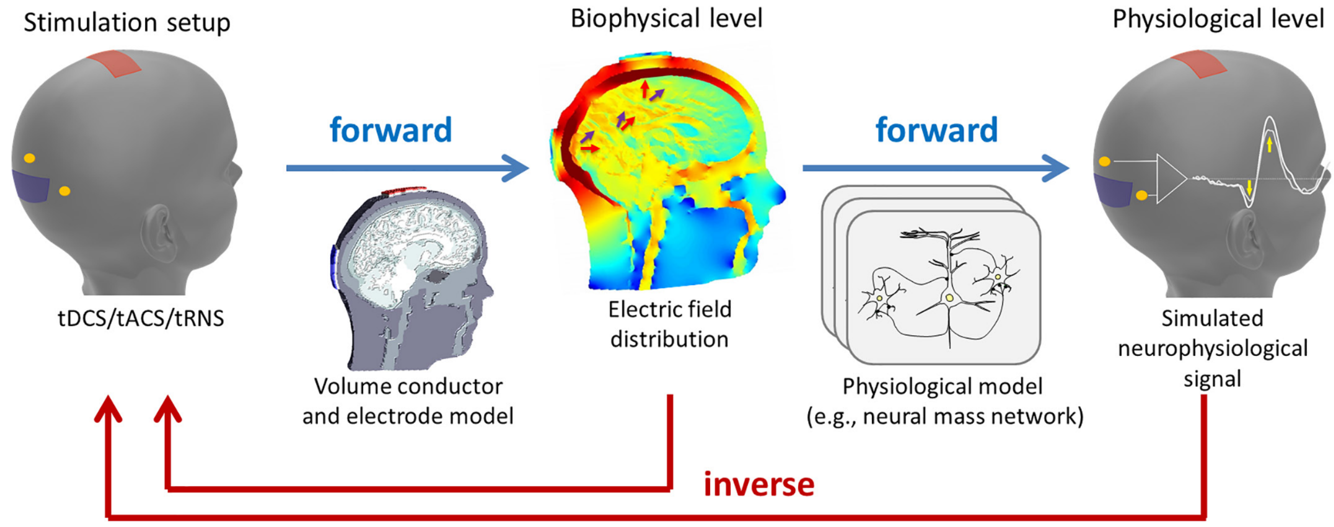

FIGURE 1 Structure of the forward and inverse problem setup for tES. A stimulation setup is shown in the left panel with an anode (red) and a cathode (blue) and two EEG electrodes (yellow). With the help of a volume conductor model and an electrode model the distribution of the electric field is computed (middle panel, field amplitude color coded). Consider, for example, three regions of interest in the brain forming a network (location and main orientation indicated by the purple arrows) for which we obtain the electric current flow characterized by an amplitude and orientation (red arrows). Note that the two orientations do not necessarily align. Neural activity can be described on a physiological level as arising from networks of interacting neurons or neural populations. For example, one may use models of interconnected neural masses. The activity in these models is modulated by tES and can be formulated in a way that they predict the activity, for example, measured by the EEG during an experiment (right panel). The inverse methods seek to invert these forward models, trying to estimate optimal electrode parameters (e.g., number, size, and positions) and/or stimulation current parameters (e.g., amplitude, frequency, and/or signal forms).

regions and unwanted stimulation at nontarget regions. Even optimization on single targets essentially results in a compromise between stimulation intensity at the target and the field throughout the brain (Dmochowski et al., 2011). Without restricting, for example, the intensity, also nontarget regions will receive field intensities, that might be sufficient to induce modulation effects (Gomez-Tames et al., 2020).

The head models applied in current flow modeling can be extended with models of neurons or neuronal populations representing brain activity and interacting in networks. The simulated induced field at a considered region is used as modulatory input to such neuronal models mimicking stimulation effects on the neuronal dynamics which in turn can be used to compute neurophysiological quantities such as the EEG (Kunze et al., 2016), see Figure 1. Ultimately, these neurophysiological quantities can be linked to behavioral effects or treatment responses.

Previous reviews summarized current flow modeling studies for single (Bikson et al., 2012) and multichannel (Miranda et al., 2018) tES setups with a focus on the methodological strategy covering the pipeline from individual image datasets, over model parameters to the electric field simulation and incorporated other sources of behavioral variability in terms of state-dependent and contextual factors (Vergallito et al., 2022).

In line with these preceding reviews summarizing modeling aspects and sources of variability in tES effects, in this minireview, we build upon an updated literature search. We used the terms "transcranial electrical stimulation" and "current flow model" or "electric field model" and "behavioral effect" or "physiological effect" to foster the databases of PubMed, the Web of Science, and Google Scholar. During the selection of studies for this minireview, we focused on studies that investigated the association between current flow modeling features and the characteristics of behavioral or neurophysiological responses (for an overview see Table 1).

2 | CURRENT FLOW MODELING IN GENERIC AND INDIVIDUAL MODELS

Simulations of the current flow rely on models of the head (which are also called volume conductor models) and models of the electrodes. Initially, spherical head models representing the scalp, skull, and brain compartments as nested spheres were utilized (Bikson et al., 2008; Miranda et al., 2006) to infer the electric field intensity and orientation impressed by different stimulation electrode configurations. A first realistically shaped model based on magnetic resonance imaging (MRI) data approximated the head geometry with scalp, skull, cerebrospinal fluid (CSF), gray and white matter to demonstrate different intensity distributions in brains containing lesions (Wagner et al., 2007). Following this line of modeling, tissue compartments of the scalp, skull, CSF, and brain were segmented from an MRI dataset of one person (Datta et al., 2009). This model was used to show the difference in focality between a bipolar and a distributed montage of four anodes and one central cathode. The terminology for the

TABLE 1 Overview of the cited original studies, which investigate a relationship between current flow modeling and physiological effects of tES

Reference	Participants age: Mean ± SD (or age range) study design task/ measurements	Stimulation parameters	Modell generic/ individual	Software	Retrospective/ prospective	Main results
Albizu et al. (2020). *Brain Stimulation*	Healthy $N = 14$. Age: 73.57 ± 7.84 control sham group. 2-week cognitive training intervention during tDCS. N-back working memory task pre-/post-intervention	tDCS: 2 mA 20 min. Rectangular electrodes 5×7 cm^2 F3 (cathode)-F4 (anode)	Individual	ROAST	Retrospective	SVM models of tDCS current components had 86% overall accuracy in classifying treatment responders versus nonresponders, with current intensity producing the best overall model differentiating changes in working memory performance. Median current intensity and direction in brain regions near the electrodes were positively related to intervention responses
Antonenko et al. (2022). *Alzheimer's & Dementia: Translational Research & Clinical Interventions*	Healthy $N = 51$. Age: 70 ± 4 single-blind randomized controlled trial comparing cognitive training to concurrent anodal tDCS or sham. Markov decision-making tasks; N-back	tDCS: 1 mA, 20 min round electrodes, ⌀5 cm; F3(anode)–Fp2	Individual	SimNIBS	Retrospective	No between-group differences emerged in the trained letter updating and Markov decision-making tasks at post-intervention and at follow-up timepoints. Secondary analyses revealed group differences in one near-transfer task: Superior n-back task performance was observed in the tDCS group at post-intervention and at follow-up. Improvements in working memory were associated with individually induced electric field strengths
Antonenko et al. (2019). *Brain Stimulation*	Healthy $N = 24$. Age: 25 ± 4 Randomized, sham-controlled, crossover study. Pre–post-MRS	tDCS: 1 mA, 15 min. rectangular electrodes 5×7 cm^2 C3 (anode)- right SO (cathode)	Individual	SimNIBS	Retrospective	On a neurophysiological level: the expected reduction of GABA concentrations and increase in sensorimotor network strength, both during anodal and cathodal compared to sham tDCS. The magnitudes of neurophysiological modulations induced by tDCS were significantly associated with simulation-based electric field strengths within the targeted left precentral gyrus

TABLE 1 (Continued)

Reference	Participants age: Mean ± SD (or age range) study design task/ measurements	Stimulation parameters	Modell generic/ individual	Software	Retrospective/ prospective	Main results
Cabral-Calderin et al. (2016). *Neuroimage*	Healthy *N* = 20. Age: 25.1 ± 3.1 Randomized, sham-controlled, simultaneous fMRI-tACS crossover study. fMRI signal fluctuations (pre–post)	tACS: 1 mA. 8 min at 10, 16, 40 Hz, different montages. Round electrodes 16 cm^2 Cz–Oz; P5–P6	Individual	SimNIBS	Retrospective	EF simulations showed that tACS over Cz–Oz directly stimulates occipital cortex, while tACS over P5–P6 primarily targets parietal cortices. Group-level simulation-based functional connectivity maps for Cz–Oz and P5–P6 resembled the visual and fronto-parietal control resting-state networks, respectively. The effects of tACS were frequency and partly electrode montage dependent. In regions where frequency-dependent effects of tACS were observed, 10 and 40 Hz tACS generally induced opposite effects
Caulfield et al. (2020). *Brain Stimulation*	Healthy *N* = 29. Age: 26.9 ± 9.1 Visit 1 MT measurements Visit 2: anatomical MRI	Individualized tDCS. Dosage range: 3.75–9.74 mA to produce 1 V/m over M1	Individual	SimNIBS	Retrospective	The tES MT, but not the TMS-MT, significantly correlated with the ROI-based reverse-calculated tDCS dose determined by EF modeling
Caulfield et al. (2022). *Neuromodulation*	Healthy *N* = 28. Age: 73.7 ± 7.3 tDCS (*N* = 14) sham (*N* = 14). Randomized, sham-controlled triple-blind design. The primary behavioral outcome measure was accuracy on a 2-Back Letter Task	tDCS: 2 mA rectangular electrodes, 5 × 7 cm^2 F3 (cathode)-F4 (anode)	Individual	SimNIBS	Retrospective	Working memory improvements from pre- to post-tDCS were significant for the above-median electric field from active 2 mA condition at the left DLPFC. The reverse-calculation modeling significantly reduced electric field variance at both left and right DLPFC
Gbadeyan et al. (2019). *Journals of Gerontology: Psychological Sciences*	Healthy *N* = 36. Age: 66.02 ± 6.92 The double-blind, sham HD-tDCS controlled, crossover design. HD-tDCS during a visual flanker task	tDCS 1 mA, 20 min F4 (anode ⃠2.5 cm)—Cathode: a ring-shaped electrode, symmetrically around the anode ⃠11.5 cm	Generic	SimBio	Retrospective	Active HD-tDCS enhanced Conflict adaptation in older adults. Current modeling analysis demonstrated focal current delivery to the DLPFC with sufficient magnitude of the induced current to modulate neural function in older adults

(Continues)

TABLE 1 (Continued)

Reference	Participants age: Mean ± SD (or age range) study design task/ measurements	Stimulation parameters	Modell generic/ individual	Software	Retrospective/ prospective	Main results
Indahlastari et al. (2021). *Brain Stimulation*	Healthy *N* = 15. Age: 71.8 (61–82) Randomized, double-blinded sham-controlled, crossover study. During tDCS-fMRI participants performed a series of N-Back tasks	tDCS: 2 mA, 12 min. Rectangular electrodes 5×7 cm^2 F4(anode)–F3(cathode)	Individual	Simpleware/ COMSOL	Retrospective	The amount of current within the left DLPFC ROIs was found positively correlated with changes in functional connectivity between left DLPFC and left VLPFC during active 2 mA stimulation
Indahlastari et al. (2018) *Neural Plasticity*	Healthy *N* = 6. Age: 24 (20–39) The subjects underwent 10 Hz tACS while being imaged in an MRI scanner. They ratings of phosphene experience were collected during tACS and compared against current density distributions predicted in eye and occipital lobe ROIs determined for each subject	tACS (10 Hz), 1.5 mA, different montages. Rectangular electrodes 5×5 cm^2 T7–T8 Fpz–Oz	Individual	Simpleware/ COMSOL	Retrospective	Higher current densities in the eyes were consistently associated with decreased phosphene generation for the Fpz–Oz montage. There was an overall positive association between phosphene perceptions and current densities in the occipital lobe
Jamil et al. (2020). *Hum Brain Mapp*	Healthy *N* = 29. Age: 25 ± 4.4 29 participants divided into two groups, anodal or cathodal tDCS. For each group randomized, sham-controlled, single-blind crossover design. (1) Changes in TMS-induced MEP (tDCS-TMS-MEP) and (2) changes in cerebral blood flow (CBF) measured by fMRI, for up to 2 h after intervention	tDCS: anodal or cathodal .5 mA, 1 mA, 1.5 mA, 2 mA. 15 min. Rectangular electrodes M1 (active: 5×7 cm^2)- Right orbit (refernce:10×10 cm^2)	Generic	SimNIBS	Retrospective	ROI analyses indicated linear intensity- and polarity-dependent tDCS after-effects: all anodal-M1 intensities increased CBF under the M1 electrode, with 2.0-mA increasing CBF the greatest (15.3%) compared to sham, while all cathodal-M1 intensities decreased left M1 CBF from baseline, with 2.0-mA decreasing the greatest (−9.3%) from sham after 120 min. The spatial distribution of perfusion changes correlated with the predicted electric field, as simulated with finite element modeling

JOURNAL OF Neuroscience Research

TABLE 1 (Continued)

Reference	Participants age: Mean ± SD (or age range) study design task/ measurements	Stimulation parameters	Modell generic/ individual	Software	Retrospective/ prospective	Main results
Kasten et al. (2019). *Nature Communications*	Healthy In two experiments, participants received 20 min of either α-tACS (1 mA) or sham stimulation. Experiment 1: $N = 40$. Age: 24 ± 3 randomly assigned to one of two experimental groups (tACS or sham) in a single-blind design. Experiment 2: $N = 19$. Age: 25 ± 3 volunteers received tACS or sham stimulation on one of two experimental sessions on separate days. The order of stimulation conditions was counterbalanced across participants. MEG was recorded for 10 min before and after stimulation	tACS: 1 mA, individual alpha peak frequency 20 min. Rectangular electrodes Cz ($7 \times 5\,cm^2$)–Oz ($4 \times 4\,cm^2$)	Individual	ROAST	Retrospective	tACS caused a larger power increase in the α-band compared to sham. The variability of this effect was significantly predicted by measures derived from individual electric field modeling
Kim et al. (2014). *Neuroscience Letters*	Healthy $N = 17$. Age: 22.2 ± 1.4 A 3-back verbal WM task was conducted before and after tDCS. Participants were classified into two categories based on behavioral indices of the WM tasks: a group of individuals who showed a positive tDCS after-effect and the other group of individuals who did not show any significant enhancement in behavioral outcomes	tDCS: 1 mA. 20 min. Rectangular electrodes $5 \times 7\ cm^2$ F3 (anode)- right SO (cathode)	Individual	COMETS	Retrospective	The results showed that participants who showed evidence of enhanced WM task performance after tDCS had a significantly larger current density at the DLPFC than other participants, suggesting that inconsistent behavioral outcomes of tDCS might be partly due to individual anatomical differences
Laakso et al. (2019). *Scientific Reports*	Healthy $N = 28$. Age: 27 ± 6 Randomized, sham-controlled, double-blind crossover study. TMS-MEP before after 0–30 min (with 10 min intervals) after tDCS	tDCS: 1 mA, 20 min. Rectangular electrodes $5 \times 5\,cm^2$ rightM1 (anode)-contralateral orbit (cathode)	Individual	Inhouse	Retrospective	The results demonstrate that a large part of interindividual variability in tDCS may be due to differences in the electric fields

(Continues)

TABLE 1 (Continued)

Reference	Participants age: Mean ± SD (or age range) study design task/ measurements	Stimulation parameters	Modell generic/ individual	Software	Retrospective/ prospective	Main results
Mendonca et al. (2011). *The Journal of Pain*	Pain Patients $N = 30$. Age: 43.2 ± 9.8 Randomized, double-blind clinical trial. The patients were randomized into five groups (Cathodal-M1, Cathodal-SO Anodal-M1, Anodal-SO, and Sham) to receive tDCS application using an extracephalic montage. Pain was measured using VNS, PPT and a body diagram evaluating pain area	tDCS 2 mA, 20 min, different montages. Rectangular electrodes. M1 (cathode: $4 \times 4\,cm^2$)- Reference: extracephalic position $8 \times 10\,cm^2$ M1 (anode $4 \times 4\,cm^2$)- Reference extracephalic position $8 \times 10\,cm^2$ SO-M1	Generic	Simpleware/ COMSOL	Retrospective	There was significant pain reduction in cathodal-SO and anodal-SO groups indexed by VNS. For PPT there was a trend for a similar effect in anodal-SO group. Computer simulation indicated that the M1-extracephalic montage produced dominantly temporo-parietal current flow, consistent with lack of clinical effects with this montage. Conversely, the SO-extracephalic montage produced current flow across anterior prefrontal structures, thus supporting the observed analgesic effects. Our clinical and modeling findings suggest that electrode montage, considering both electrodes, is critical for the clinical effects of M1-tDCS as electric current needs to be induced in areas associated with the pain matrix
Meier et al. (2019). *PLoS One*	Healthy $N = 26$. Age: 28.5 ± 7.9 Randomized, sham-controlled, single-blind crossover study. HD-tACS during a dichotic listening task. EEG was recorded during resting state (before/after) and during stimulation (sham/verum) At the behavioral level: Task performance during sham- and verum-tACS. At the EEG level: EEG-Task analyses on the sham session	Multisite HD-tACS: 1 mA, 40 Hz for 20 min. Ag/AgCl circular electrodes ⦸12 mm Electrode placement was based on a current flow model, which was optimized to target the auditory cortex based on 40 available electrode positions	Generic	Inhouse	Prospective	The results demonstrate that 180°-tACS did not affect the right ear advantage during a dichotic listening task at group level. However, a follow-up analysis revealed that the intrinsic phase asymmetries during sham-tACS determined the directionality of the behavioral modulations: While a shift to left ear percept was associated with augmented interhemispheric asymmetry (closer to 180°), a shift to right ear processing was elicited in subjects with lower asymmetry (closer to 0°). Crucially, the modulation of the interhemispheric network dynamics depended on the deviation of the tACS-induced phase lag from the intrinsic phase asymmetry

TABLE 1 (Continued)

Reference	Participants age: Mean ± SD (or age range) study design task/ measurements	Stimulation parameters	Modell generic/ individual	Software	Retrospective/ prospective	Main results
Mosayebi-Samani et al. (2021). *Brain Stimulation*	Healthy $N = 29$. Age: 25.0 ± 4.44 Participants divided into two groups, anodal ($N = 15$) or cathodal ($N = 14$) tDCS. For each randomized, sham-controlled, single-blind crossover study. (1) Changes in TMS-induced MEP (tDCS-TMS-MEP) and (2) changes in cerebral blood flow (CBF) measured by fMRI, for up to 2 h after intervention	tDCS: anodal or cathodal .5, 1; 1.5, 2 mA. 15 min. Rectangular electrodes M1 (active: $5 \times 7\,cm^2$)- Right orbit (refernce:$10 \times 10\,cm^2$)	Individual	Simpleware/ COMSOL	Retrospective	The results highlight a significant negative correlation between regional electrode-to-cortex distance as well as regional CSF thickness, and the individual EF characteristics. In addition, while both rCSF thickness and rECD anticorrelated with tDCS-induced physiological changes, EFs positively correlated with the effects
Muffel et al. (2019). *Frontiers in Aging Neuroscience*	Healthy $N = 21$. Age: 27.0 ± 2.4 $N = 24$. Age: 69.4 ± 4.9 Crossover, double-blind experiment in both age groups. Proprioceptive accuracy task.	tDCS: 1 mA, 20 min. Rectangular electrodes S1 (anode $5 \times 5\,cm^2$)- Fp2 (cathode $7 \times 5\,cm^2$)	Generic	SimNIBS	Retrospective	Anodal-tDCS elicited differential changes in proprioceptive accuracy and EF strengths in the two groups: while young adults showed a slight improvement, old adults exhibited a decrease in performance during a-tDCS. Stronger EFs were induced in target S1 and control areas in the young adults. However, no relationship between EF strength and performance change was found
Rasmussen et al. (2021). *Journal of Alzheimer's disease: JAD*	Alzheimer's disease $N = 19$. Age: 72.58 ± 7.19 Double-blind, sham-controlled, parallel-group trial. Delayed verbal memory and Mini Mental Status Examination	HD-tDCS-induced electric field in each patient's brain. 2 mA for 3×20 min	Individual	SimNIBS	Prospective	Different montages were optimal for individual patients in terms of the electric field distribution in the brain. The active HD-tDCS group improved significantly in delayed memory and Mini Mental Status Examination performance compared to the sham group. Associations between the delayed memory effect of HD-tDCS and both E-field and cortical thickness were observed

(Continues)

TABLE 1 (Continued)

Reference	Participants age: Mean ± SD (or age range) study design task/measurements	Stimulation parameters	Modell generic/individual	Software	Retrospective/prospective	Main results
Splittgerber et al. (2021). *Scientific Reports*	Healthy $N = 22$. Age: 15.18 ± 1.9 Randomized, sham-controlled, double-blind crossover study. Stimulation with and without a 2-back task. After stimulation, the 2-back task and a Flanker task were performed. Resting state and task-related EEG were recorded	tDCS 2 mA (total inject current), 20 min Five 3.14 cm^2 circular electrodes over left DLPFC	Individual	COMSOL	Retrospective	Performance and neurophysiological activity in the 2-back task were not affected by atDCS. atDCS reduced reaction times in the Flanker task, independent of whether atDCS had been combined with the 2-back task. Flanker task-related beta oscillation increased following stimulation without 2-back task performance Anodal tDCS effects were not correlated with the E-field
Splittgerber et al. (2020). *Frontiers in Human Neuroscience*	Healthy $N = 24$. Age: 24.8 ± 2.7 Randomized, sham-controlled, single-blind crossover study. Stimulation with a 2-back task. After stimulation, EEG was recorded during 2-back and nontarget continuous performance task. Resting state EEG before and after stimulation	tDCS. Different montages 1 mA, 20 min circular electrodes F3(anode 25 cm^2)–Fp2(cathode 25 cm^2). tDCS 2 mA (total inject current), 20 min over DLPFC. Five 3.14 cm^2circular electrodes over left DLPFC	Generic	COMSOL	Retrospective	For multichannel stimulation, initially low-performing participants tended to improve their WM performance, while initially high-performing participants tended to worsen their performance compared to sham stimulation. Both tDCS montages induced changes in neural oscillatory power, which correlated with baseline performance. The worse the participants' initial WM performance was, the more task-related theta power was induced by multichannel and bipolar stimulation. The same effect was observed for alpha power in the nontarget task following multichannel stimulation
Suen et al. (2021). *European Archives of Psychiatry and Clinical Neuroscience*	Major depression $N = 16$. Age: 18–75 Double-blind, sham-controlled study. Primary Outcome Measures changes in HDRS-17; changes in affective scores and in trait or state anxiety measured by the State–Trait Anxiety Inventory	tDCS: 2 mA 30 min rectangular electrodes 5×5 cm^2 F5-F6	Individual	SimNIBS	Retrospective	EF strength was inversely associated with negative affect in the bilateral ACC and with depression scores in the left ACC EF strength in the left ACC was correlated with changes in HDRS-17. No association between positive affect or anxiety scores, and simulated EF strength in the investigated brain regions was found

TABLE 1 (Continued)

Reference	Participants age: Mean ± SD (or age range) study design task/ measurements	Stimulation parameters	Modell generic/ individual	Software	Retrospective/ prospective	Main results
Suzuki et al. (2022) *Brain Science*	Healthy *N* = 16. Age: 25.1 ± 7.5 a single-center, single-blinded, within-participant study. MEPs, short-interval intra-cortical inhibition (SICI) and EEG (power changes) measurements, measurements before and after tACS	tACS: .6 mA. 20 min at 10, 20 Hz, or sham. Two rubber electrodes 1.8 × 1.8 cm^2 Cz–CP1. Montage selection based on a group level analysis of the electric field strength in the precentral knob	Generic	Inhouse	Prospective	Results indicated that 10 and 20 Hz tACS resulted in larger alpha and beta oscillations, respectively, compared with the oscillations observed after sham-tACS. In addition, 10 and 20 Hz-tACS decreased the amplitudes of conditioned MEPs and increased alpha and beta activity, respectively. Correspondingly, alpha- and beta-tACSs enhanced cortical inhibition. tACS frequency differentially affects motor cortex oscillation and inhibition
Zanto et al. (2021) *Brain Stimulation*	Healthy *N* = 60. Age: 60–80 control group 1-Hz tACS. A multitasking paradigm, NeuroRacer was conducted with concurrent tACS. Each participant was assessed on 5 consecutive days and then again 1 month later	tACS 2 mA peak to peak. 6 or 1 Hz. 16 or 26.7 min. Circular electrodes 3.14 cm^2 F3–F4	Individual	ROAST	Retrospective	Results indicated that only in the Long Theta group, performance change was correlated with modeled EF and peak theta frequency. Together, modeled EF and peak theta frequency accounted for 54%–65% of the variance in tACS-related performance improvements, which sustained for a month

Abbreviations: ACC, anterior cingulate cortex; DLPFC, dorsolateral prefrontal cortex; EEG, electrode positions according to the 10–20 System; EF, Electrical field; HDRS-17, Hamilton depression rating scale; HD-tDCS, high definition transcranial direct current stimulation; M1, primary motor cortex; MEP, Motor evoked potential; MRS, magnetic resonance spectroscopy; MT, motor threshold; PPT, pressure pain threshold; ROI, regions of interest; S1, primary somatosensory cortex; SO, Supraorbital; SVM, Support Vector Machine; TES, transcranial electrical stimulation; TMS, transcranial magnetic stimulation; VLPFC, ventrolateral prefrontal cortex; VNS, Visual Numerical Scale; WM, working memory.

current flow modeling and simulation was introduced by Sadleir et al. (2010) and the modeling approaches were first summarized by Bikson et al. (2012). Rampersad et al. (2014) proposed a model that included scalp, compact and spongy bone, CSF, gray and anisotropic white matter which was based on T1, T2, and diffusion-weighted MRI datasets. Simulations with several models have been performed for individuals in different developmental stages (Kessler et al., 2013) and with pathological conditions that affect the head geometry (Truong et al., 2013). To compare simulation results derived from individual models, the cortical surfaces were mapped into a standard space, for example, the Montreal Neurological Institute (MNI) template brain (Laakso et al., 2016; Opitz et al., 2015). Also, generic head models have been proposed (Huang et al., 2016). Recent studies with advanced individual head models suggest that current flow in a cortical target can predict the efficacy of transcranial electrical stimulation (Albizu et al., 2020; Kasten et al., 2019; Laakso et al., 2019). Their data emphasize the impact of individual brain anatomy on the impressed field intensity and spread, and support the usefulness of numerical estimations of the electric field to make predictions on the empirical efficacy.

The methodology of current flow modeling was verified in surgical patients (Huang et al., 2017; Opitz et al., 2016), human cadavers (Vöröslakos et al., 2018), and physical phantoms (Jung et al., 2013; Kim et al., 2015) by comparing simulated and measured electric fields.

A central question when planning a tES study is the one about the methodology for current flow modeling. There are several levels of modeling detail (from simple spheres to realistic compartments and detailed voxel models) and several methods for computation (e.g., semi-analytical, boundary element, finite difference, and finite element methods) available. The choice needs to consider three main factors: accuracy, information availability, and modeling/computation costs. Of course, an analytical multi-sphere model is less accurate in terms of the approximation of the head geometry and, in consequence, the electric field estimation, than a realistically shaped numerical model. However, more realistic models tend to require more detailed information in terms of head geometry and material properties. The availability of individual MRI scans is not always given and thus scaled generic realistic models might be used in these cases. In case of only partially available individual data, for example, in case of a limited field of view, another approach lies in the construction of fused models with extensions of, for example, the neck from averaged data (Gomez-Tames et al., 2019). Using realistic models necessitates the availability and segmentation of image data of the head. The full advantage of finite element over boundary element models is only effective if (possibly anisotropic) conductivity information is available on a voxel or at least on a region base. Realistic volume conductor models tend to be more costly, not only during the computation but also during model generation, with the latter being the more important part. Nevertheless, individually shaped compartment models represent the current state of the art.

There are multiple software toolboxes to perform current flow modeling, which include freely available tools: SimNIBS (Windhoff et al., 2013), ROAST (Huang et al., 2019), SCIRun (Dannhauer et al., 2012), COMETS (Lee et al., 2017), SimBio (Wagner et al., 2014); in-house pipelines (Laakso & Hirata, 2013) and commercial software: Simpleware/COMSOL (Datta et al., 2011), HD-Explore/HD-Targets (Soterix Medical Inc., Woodbridge, USA), and tES LAB (Neurophet Inc., Seoul, Republic of Korea).

3 | INDUCED FIELD AND STIMULATION MONTAGE BASED ON INDIVIDUAL MODELING

A cognitive training study with a group of elderly participants did not show an expected effect of tDCS on task performance when applying a protocol with 1 mA current intensity, derived from studies with young participants (Antonenko et al., 2022). The authors indicate signs of atrophy in their retrospectively analyzed head models for current flow modeling and indicated the missing correction for effective electric field strength as a compromising factor on the stimulation results. A meta-analysis of prefrontal tDCS effects on working memory performance was based on a performance—electric field correlation (PEC) associating behavioral effect size to tDCS-induced electric field strength (Wischnewski et al., 2021). Different stimulation configurations including both electrode configurations and stimulation intensities addressing tDCS effects on working memory were simulated in a generic head model. The authors found a positive correlation between induced electric field strength and reported behavioral effect size. Furthermore, the authors used the location with maximal PEC as the target for a tDCS optimization in the generic head model to guide future attempts addressing tDCS-induced working memory effects (Wischnewski et al., 2021). Similarly, a retrospective analysis of simulated electric field strength in depressed patients who received tDCS indicated a positive correlation between high electric field strength in prefrontal cortical areas and improvements in the behavioral outcomes (Suen et al., 2021). Comparing the electric field strength from 2 mA tDCS in the dorsolateral prefrontal cortex (DLPFC) of healthy older participants to improvements in working memory performance indicated the correspondence of higher behavioral effects to higher cortical electric field strength. Thus, the authors suggested simulating the stimulation intensity necessary to achieve an effective cortical electric field strength (Caulfield et al., 2022). An individual selection of the stimulation montage targeting the DLPFC with 4 × 1 montages relied on current flow modeling in individual head models from Alzheimer's disease patients (Rasmussen et al., 2021). In this study, the selection of the stimulation electrode configuration was based on the prediction of the highest anodal electric field strength in the left DLPFC. The individually adapted stimulation montage resulted in significantly improved delayed memory in the patients who received a higher mean electric field strength (.07 V/m) versus patients with a lower mean electric field strength (.05 V/m). This difference of approx. 28.5% in net electric field strength was linked to an effect size of

.78 and thus supports the increase in the tES efficacy based on individual current flow modeling, taking the effective intensity into account. Similarly, Suzuki et al. (2022) selected the electrode montage for tACS of the motor cortex based on individual modeling and used a group-level analysis of the electric field strength in the precentral knob. They identified the montage Cz–CP1 to produce the most intense (factor 2) and least variable (factor 4) electric field intensity in the target area. Consequently, they used this stimulation montage to modulate conditioned and unconditioned motor evoked potentials (MEPs) by tACS with 10 Hz and 20 Hz and found different tACS frequencies to change cortical inhibition, as identified in the MEP recordings.

Klaus and Schutter (2021) investigated the electric field strength and spread of large conventional and small alternative two-electrode montages for targeting the right posterior cerebellum with tDCS. In this study, interindividual and montage differences in the achieved maximum field strength, focality, and direction of current flow were evaluated in 20 individual head models. The findings suggest that compared to several conventional montages, the electric field strength in extra-cerebellar regions is significantly reduced by placing smaller electrodes in closer vicinity of the targeted area.

The importance of individual current flow modeling is also supported by studies investigating optimization methods for multichannel tDCS in adults and also in children and adolescents (Khan et al., 2021; Salvador et al., 2021; Splittgerber et al., 2021).

A comparison of different stimulation montages incorporating bipolar setups with large rectangular patch electrodes and small circular electrodes, as well as 4×1 montages (four cathodes surround one central anode) revealed interindividual variability and the predicted electric field strengths to be correlated with the focality of the electric field strengths (Mikkonen et al., 2020). This labels individual modeling as influential for proposing more specific stimulation montages leading to more focal cortical electric field strength profiles.

A multichannel montage was optimized for electric field direction parallel to assumed dipoles in Brodmann area 42, mirrored at the midline and tACS stimulation was provided with 180 degree phase shift to the left and right auditory cortex (Meier et al., 2019). With this fixed stimulation setup, the authors modulated interhemispheric auditory processing. The efficacy of multichannel tACS for improving working memory in older adults was demonstrated by stimulating the prefrontal and temporal regions with different stimulation intensities. Stimulation intensities were based on current flow modeling that determined comparable electric field strengths for the prefrontal regions at .6 mA and the temporal regions at 1.0 mA (Reinhart & Nguyen, 2019).

The importance of the selection of stimulation intensities was also shown in a further multichannel tACS study (Tan et al., 2020), suggesting that targeting nonhomologous regions should use current flow modeling to determine stimulation intensities that provide comparable electric field strengths for the targeted stimulation sites.

Multiple tACS channels with different sinusoidal frequencies are superimposed to result in a temporal interference, whereas the amplitude of the electric field beats with the frequency difference between the tACS channels and is meant to generate more focally effective electric fields (cf. (Grossman et al., 2017) for details). A recent study performed simulations of temporal interference tES (TI-tES) with the aim to derive individually optimized electrode montages for three persons such that a targeted region receives maximum stimulation (Lee et al., 2020). The authors revealed different electrode montages and stimulation intensity distributions on the two TI-tES channels for the three different individual head models. On the contralateral side, an electrode at position PO7 was commonly involved in the stimulation channel with the higher stimulation current, which was completed with an electrode at F7, FC3, or FC5. On the ipsilateral side, the stimulation channel with the lower stimulation channel incorporated T8–F8 or P8–FC6. This diversity in the montages underlines the importance of individual current flow modeling.

Clinical evaluation was combined with current flow modeling in a representative model to investigate the effects of different montages in clinical conditions such as fibromyalgia (Mendonca et al., 2011). For each electrode montage, clinical effects were correlated with predictions of induced cortical current density using a single MRI-derived finite element method head model. Their findings suggest that the electrode montage is critical for the clinical effects of tDCS as electric current needs to be delivered to areas associated with the pain matrix. In stroke patients, Dmochowski et al. (2013) found a 64% increase in electric current in a cortical target and a 38% improvement in a behavioral task using individualized electrode montages based on individualized MRI-based modeling.

4 | ANATOMICAL REPRESENTATION AS A DETERMINANT FOR STIMULATION EFFICACY

Anatomical parameters, for example, the thickness of the CSF layer and the distance from the electrode to the cortex, have been directly linked to the electric field strength in the cortex with a negative correlation (Hunold et al., 2021). On the contrary, physiological effects, for example, MEPs and cerebral blood flow (CBF), were positively correlated with the tES-induced electric field strength in the cortex (Mosayebi-Samani et al., 2021). Their study established a direct link between tissue thickness via a negative correlation of induced electric field strength and the tES-induced physiological effects on MEP and CBF. Similarly, the electric field strength calculated in the DLPFC of individual head models for an F3–Fp2 stimulation with 1 mA corresponded to the classification of positive and neutral effects on working memory in these individuals (Kim et al., 2014). Caulfield et al. (2020) found a positive correlation between the motor threshold of tES and the estimated stimulation intensity to reach an electric field intensity of 1 V/m in the cortex underneath the anode. In the eye, as a distinct target subsystem, studies comparing current flow modeling results and phosphene perception indicated good agreement of current density intensity in the retina and perceived phosphenes for transcranial stimulation at electrode positions T7–T8 (Indahlastari et al., 2018) and transorbital stimulation (Sabel et al., 2021), indicating simulated current flow as a marker for physiological stimulation effects. The study by Indahlastari and colleagues indicated a significant correlation between simulated current density and functional connectivity in a cohort of healthy elderly participating in a working memory task (Indahlastari et al., 2021).

Another approach to represent anatomical features is based on group properties using the head circumference (Antonenko et al., 2021) or age (Ciechanski et al., 2018; Gbadeyan et al., 2019; Hunold et al., 2021; Muffel et al., 2019) as a marker for implication on net stimulation intensity in the brain.

Current flow models, reflecting anatomical characteristics, are especially relevant for safety and effectiveness considerations when fractions of the skull as the main conductivity barrier are missing or filled with non-bone material (Datta et al., 2010; Sun et al., 2021). Also, the brain as the site of action can demonstrate pathological features like atrophy (Albizu et al., 2020; Antonenko et al., 2022) and lesions (Datta et al., 2011; Kalloch et al., 2020; Piastra et al., 2021), which affect the electric field propagation and thus the effective stimulation intensity. These studies, showing the importance of specific defect/lesion modeling, indicate that tES findings cannot be arbitrarily generalized. Supporting this statement, a tACS study on multitasking performance in older healthy adults failed to transfer stimulation effects from young healthy adults when applying the same stimulation configuration (Zanto et al., 2021). Specifically, individual current flow modeling for the older adults revealed considerable interindividual differences in the tACS-induced cortical electric field spread, which correlated with the multitasking performance in such a way that the highest induced electric field strength was linked to the greatest improvements in multitasking performance. Furthermore, pronounced differences in the individual intensity level might be caused by brain atrophy. Even though aging is a prominent way leading to brain atrophy, the current intensity at the cortical level did not correlate well with age in older adults but with the individual level of atrophy (Indahlastari et al., 2020).

In addition to anatomical features, also the conductivity values of the tissues in the head affect the propagation of the stimulation current and thus the cortical electric field intensity and spread. Investigations on the influence of uncertainty in the tissue's conductivity values revealed considerable effects on the electric field in the gray matter (Saturnino, Thielscher, et al., 2019; Schmidt et al., 2015). These studies identified the conductivity values of the scalp and the skull to be most influential on the electric field intensity and spread and thus of the highest interest for individual modeling.

5 | LIMITATIONS AND FUTURE DIRECTIONS

Individual current flow modeling takes anatomical differences into account and therefore supports the understanding of the variability in response to tES. At present, the optimal stimulation parameters remain largely unknown, making it difficult to ensure optimal treatment response on an individual basis. A considerable research effort is still needed to obtain more clinically relevant stimulation outcomes (Bikson et al., 2018).

The electrode configuration largely determines the distribution of the intensity and the orientation of the induced electric field. The intensity and orientation of the induced electric field in the brain determine whether or not it results in an effective neural stimulation in a specific area. In this line, frontal (Manenti et al., 2017) and parietal (Crossman et al., 2019) stimulation montages have been shown to address different functional nodes in the memory reconsolidation network and working memory (Johnson et al., 2022; Jones et al., 2020). To achieve the anticipated stimulation effect, the induced field needs to reach effective intensities and align in the target region. At the same time, the induced field intensity should not reach effective intensities and/or not align in nontarget regions. Therefore, current flow modeling should be employed to analyze both target and nontarget regions to identify hotspots occurring, for example, potentially in deeper brain regions as shown by Gomez-Tames et al. (2020).

Besides the stimulation intensity, also the orientation of the induced electric field determines the effectivity on the neuronal level. The electric field component along the axon produced the maximal polarization of the neuron (Rahman et al., 2013). For cortical stimulation, mainly addressing polarization of pyramidal cells oriented predominantly perpendicular to the local gray matter surface, optimizing the electric field component oriented normally to the local cortical surface might be sufficient (Laakso et al., 2016). The direction of the induced electric field relative to the neuronal orientation in the target region should be treated with just as much attention as the field intensity in current flow modeling.

Importantly, current flow modeling alone cannot predict what modulatory effects will occur, see Figure 1. Current flow models only consider the anatomical structure, not the physiological state of the brain, that is, they do not provide predictions of the physiological impact of the target (Lee et al., 2021). For example, the effects of changes associated with physiological aging are not yet known and thus represent a latent cofactor for the age correlations mentioned above. The effects of tES in the healthy human brain do not translate to patient groups in a straightforward way, simply because the brain of these patients is likely to react differently to stimulation (Bestmann & Walsh, 2017).

Broadening the modeling and simulation scope by, for example, incorporating regions of cortical atlases (Soleimani et al., 2021) neuronal mass models or networks of such models (Kunze et al., 2016) can shed light on to electrophysiological effects on individual and group levels (Kunze et al., 2016; Soleimani et al., 2021). Compartment models can represent morphological and electrophysiological properties of neurons that can explain excitability changes induced by electric field components different from the electric field component depolarizing primarily pyramidal cells oriented normally to the local cortical surface (Chung et al., 2022). Ultimately, the depolarization of neuronal model compartments can be incorporated into the goal function of tES optimization schemes.

Furthermore, the distribution of simulated electric field intensities for tDCS in a generic head model correlated with the spatial distribution polarity-dependent changes in cerebral blood flow detected in functional MRI recorded during tDCS (Jamil et al., 2020). However, the induced electric field calculated by current flow modeling does not predict the modulation of network interactions, as for example, shown by the current flow-guided functional MRI analysis of tACS effects (Cabral-Calderin et al., 2016). Predictions of physiological effects, therefore, require model extensions with dynamic neuronal representations (Fertonani & Miniussi, 2017; Miniussi et al., 2013), see Figure 1. Specifically for tACS, effects do not depend on the direct application of a specific frequency per se but on modulation of the preexisting endogenous oscillations that are coupled with the specific brain state. Accordingly, it might be helpful to personalize future tACS stimulation paradigms, by individually defining EEG patterns regarding frequency and localization of interest prior to stimulation and then tailoring the stimulation parameters (frequency and location of stimulation) accordingly (Elyamany et al., 2021; Kasten et al., 2019) similar to other stimulation modalities (Naskovska et al., 2020; Schwab et al., 2006). Electrophysiological recordings (EEG and MEG) could be valuable to observe the changes in the brain's electrical activity and to individualize the stimulation protocol (Elyamany et al., 2021; Thut et al., 2017).

6 | CONCLUSIONS

Current flow modeling allows for predictions of electric field strength and orientation induced by tES. Accurate head models derived from individual structural images are essential for computing accurate electric fields (Saturnino, Madsen, & Thielscher, 2019). There is increasing evidence of the importance of subject-specific modeling (Bikson et al., 2012). In case of lacking individual anatomical data, current flow modeling based on generic or adapted head models can be used for computing more effective doses of tES. Individualized tES application has the potential to improve tES efficiency and help overcome reproducibility issues. Current flow modeling can facilitate causal inferences on physiological and behavioral effects of tES (Bergmann & Hartwigsen, 2020; Hartwigsen et al., 2015). Consequently, current flow modeling should be employed on a more regular basis in tES studies.

AUTHOR CONTRIBUTIONS

Conceptualization, A.H., J.H., and V.M.; *Investigation*, A.H., J.H., and V.M.; *Writing – Original Draft*, A.H., J.H., and V.M.; *Writing – Review & Editing*, A.H., J.H., V.M., and F.N.; *Visualization*, A.H. and J.H.; *Funding Acquisition*, J.H. and F.N.

FUNDING INFORMATION

For this project, AH and JH, received funding from the Free State of Thuringia (2017 VF 0035, 2018 IZN 004, and 2021 FE 9098), co-financed by the European Union under the European Regional Development Fund (ERDF). This work was supported by a grant from the Deutsche Forschungsgemeinschaft (SFB1158/B03 to Frauke Nees and Herta Flor).

ACKNOWLEDGMENT

Open Access funding enabled and organized by Projekt DEAL.

CONFLICT OF INTEREST

AH is partially employed by neuroConn GmbH. The authors declare that there is no conflict of interest regarding the publication of this paper. All the authors have read the manuscript and have approved this submission.

PEER REVIEW

The peer review history for this article is available at https://publons.com/publon/10.1002/jnr.25154.

ENDNOTE

[1] Note that depending on the size and shape of the targeted brain region its orientation definition might be not straight forward.

REFERENCES

Albizu, A., Fang, R., Indahlastari, A., O'Shea, A., Stolte, S. E., See, K. B., Boutzoukas, E. M., Kraft, J. N., Nissim, N. R., & Woods, A. J. (2020). Machine learning and individual variability in electric field characteristics predict tDCS treatment response. *Brain Stimulation*, *13*(6), 1753–1764.

Antonenko, D., Grittner, U., Puonti, O., Flöel, A., & Thielscher, A. (2021). Estimation of individually induced e-field strength during transcranial electric stimulation using the head circumference. *Brain Stimulation*, *14*(5), 1055–1058.

Antonenko, D., Thams, F., Grittner, U., Uhrich, J., Glöckner, F., Li, S. C., & Flöel, A. (2022). Randomized trial of cognitive training and brain stimulation in non-demented older adults. *Alzheimer's & Dementia (New York, N. Y.)*, *8*(1), e12262. https://doi.org/10.1002/trc2.12262

Antonenko, D., Thielscher, A., Saturnino, G. B., Aydin, S., Ittermann, B., Grittner, U., & Flöel, A. (2019). Towards precise brain stimulation: Is electric field simulation related to neuromodulation? *Brain Stimulation*, *12*(5), 1159–1168.

Bergmann, T. O., & Hartwigsen, G. (2021). Inferring causality from noninvasive brain stimulation in cognitive neuroscience. *Journal of Cognitive Neuroscience*, *33*(2), 195–225. https://doi.org/10.1162/jocn_a_01591

Bestmann, S., & Walsh, V. (2017). Transcranial electrical stimulation. *Current Biology*, *27*(23), R1258–R1262.

Bikson, M., Brunoni, A. R., Charvet, L. E., Clark, V. P., Cohen, L. G., Deng, Z. D., Dmochowski, J., Edwards, D. J., Frohlich, F., Kappenman, E. S., Lim, K. O., Loo, C., Mantovani, A., McMullen, D. P., Parra, L. C., Pearson, M., Richardson, J. D., Rumsey, J. M., Sehatpour, P., … Lisanby, S. H. (2018). Rigor and reproducibility in research with transcranial electrical stimulation: An NIMH-sponsored workshop. *Brain Stimulation*, *11*(3), 465–480.

Bikson, M., Bulow, P., Stiller, J. W., Datta, A., Battaglia, F., Karnup, S. V., & Postolache, T. T. (2008). Transcranial direct current stimulation for major depression: A general system for quantifying transcranial electrotherapy dosage. *Current Treatment Options in Neurology*, *10*(5), 377–385.

Bikson, M., Rahman, A., Datta, A., Fregni, F., & Merabet, L. (2012). High-resolution modeling assisted design of customized and individualized transcranial direct current stimulation protocols. *Neuromodulation*, *15*(4), 306–314.

Brauer, H., Kadish, N. E., Pedersen, A., Siniatchkin, M., & Moliadze, V. (2018). No modulatory effects when stimulating the right inferior frontal gyrus with continuous 6Hz TACs and TRNs on response inhibition: A behavioral study. *Neural Plasticity*, *2018*, 1–11.

Cabral-Calderin, Y., Williams, K. A., Opitz, A., Dechent, P., & Wilke, M. (2016). Transcranial alternating current stimulation modulates spontaneous low frequency fluctuations as measured with fMRI. *NeuroImage*, *141*, 88–107.

Cappon, D., Jahanshahi, M., & Bisiacchi, P. (2016). Value and efficacy of transcranial direct current stimulation in the cognitive rehabilitation: A critical review since 2000. *Frontiers in Neuroscience*, *10*, 157.

Caulfield, K. A., Badran, B. W., DeVries, W. H., Summers, P. M., Kofmehl, E., Li, X., Borckardt, J. J., Bikson, M., & George, M. S. (2020). Transcranial electrical stimulation motor threshold can estimate individualized tDCS dosage from reverse-calculation electric-field modeling. *Brain Stimulation*, *13*(4), 961–969. https://doi.org/10.1016/j.brs.2020.04.007

Caulfield, K. A., Indahlastari, A., Nissim, N. R., Lopez, J. W., Fleischmann, H. H., Woods, A. J., & George, M. S. (2022). Electric field strength from prefrontal transcranial direct current stimulation determines degree of working memory response: A potential application of reverse-calculation modeling? *Neuromodulation*, *25*(4), 578–587.

Chung, H., Im, C., Seo, H., & Jun, S. C. (2022). Key factors in the cortical response to transcranial electrical stimulations—A multi-scale modeling study. *Computers in Biology and Medicine*, *144*, 105328.

Ciechanski, P., Carlson, H. L., Yu, S. S., & Kirton, A. (2018). Modeling transcranial direct-current stimulation-induced electric fields in children and adults. *Frontiers in Human Neuroscience*, *12*, 268. https://doi.org/10.3389/fnhum.2018.00268

Coldea, A., Morand, S., Veniero, D., Harvey, M., & Thut, G. (2021). Parietal alpha tACS shows inconsistent effects on visuospatial attention. *PLoS One*, *16*, e0255424.

Crossman, M., Bartl, G., Soerum, R., & Sandrini, M. (2019). Effects of transcranial direct current stimulation over the posterior parietal cortex on episodic memory reconsolidation. *Cortex*, *121*, 78–88.

Dannhauer, M., Brooks, D., Tucker, D., & MacLeod, R. (2012). A pipeline for the simulation of transcranial direct current stimulation for realistic human head models using SCIRun/BioMesh3D. In *Annual International Conference of the IEEE Engineering in Medicine and Biology Society. IEEE Engineering in Medicine and Biology Society. Annual International Conference*, *2012* (pp. 5486–5489). https://doi.org/10.1109/EMBC.2012.6347236

Datta, A., Baker, J. M., Bikson, M., & Fridriksson, J. (2011). Individualized model predicts brain current flow during transcranial direct-current stimulation treatment in responsive stroke patient. *Brain Stimulation*, *4*(3), 169–174.

Datta, A., Bansal, V., Diaz, J., Patel, J., Reato, D., & Bikson, M. (2009). Gyri-precise head model of transcranial direct current stimulation: Improved spatial focality using a ring electrode versus conventional rectangular pad. *Brain Stimulation*, *2*(4), 201–207.

Datta, A., Bikson, M., & Fregni, F. (2010). Transcranial direct current stimulation in patients with skull defects and skull plates: High-resolution computational FEM study of factors altering cortical current flow. *NeuroImage*, *52*(4), 1268–1278.

Datta, A., Truong, D., Minhas, P., Parra, L. C., & Bikson, M. (2012). Inter-individual variation during transcranial direct current stimulation and normalization of dose using MRI-derived computational models. *Frontiers in Psychiatry*, *3*, 91. https://doi.org/10.3389/fpsyt.2012.00091

Dmochowski, J. P., Datta, A., Bikson, M., Su, Y., & Parra, L. C. (2011). Optimized multi-electrode stimulation increases focality and intensity at target. *Journal of Neural Engineering*, *8*(4), 046011.

Dmochowski, J. P., Datta, A., Huang, Y., Richardson, J. D., Bikson, M., Fridriksson, J., & Parra, L. C. (2013). Targeted transcranial direct current stimulation for rehabilitation after stroke. *NeuroImage*, *75*, 12–19.

Dmochowski, J. P., Koessler, L., Norcia, A. M., Bikson, M., & Parra, L. C. (2017). Optimal use of EEG recordings to target active brain areas with transcranial electrical stimulation. *NeuroImage*, *157*, 69–80.

Elyamany, O., Leicht, G., Herrmann, C. S., & Mulert, C. (2021). Transcranial alternating current stimulation (tACS): From basic mechanisms towards first applications in psychiatry. *European Archives of Psychiatry and Clinical Neuroscience*, *271*(1), 135–156.

Evans, C., Bachmann, C., Lee, J. S. A., Gregoriou, E., Ward, N., & Bestmann, S. (2020). Dose-controlled tDCS reduces electric field intensity variability at a cortical target site. *Brain Stimulation*, *13*(1), 125–136.

Fertonani, A., & Miniussi, C. (2017). Transcranial electrical stimulation: What we know and do not know about mechanisms. *The Neuroscientist*, *23*(2), 109–123.

Fregni, F., El-Hagrassy, M. M., Pacheco-Barrios, K., Carvalho, S., Leite, J., Simis, M., Brunelin, J., Nakamura-Palacios, E. M., Marangolo, P., Venkatasubramanian, G., San-Juan, D., Caumo, W., Bikson, M., & Brunoni, A. R. (2021). Evidence-based guidelines and secondary meta-analysis for the use of transcranial direct current stimulation in neurological and psychiatric disorders. *International Journal of Neuropsychopharmacology*, *24*(4), 256–313.

Friehs, M. A., Frings, C., & Hartwigsen, G. (2021). Effects of single-session transcranial direct current stimulation on reactive response inhibition. *Neuroscience and Biobehavioral Reviews*, *128*, 749–765.

Gbadeyan, O., Steinhauser, M., Hunold, A., Martin, A. K., Haueisen, J., & Meinzer, M. (2019). Modulation of adaptive cognitive control by prefrontal high-definition transcranial direct current stimulation in older adults. *Journals of Gerontology—Series B Psychological Sciences and Social Sciences*, *74*(7), 1174–1183.

Gomez-Tames, J., Asai, A., & Hirata, A. (2020). Significant group-level hotspots found in deep brain regions during transcranial direct current stimulation (tDCS): A computational analysis of electric fields. *Clinical Neurophysiology*, *131*(3), 755–765.

Gomez-Tames, J., Asai, A., Mikkonen, M., Laakso, I., Tanaka, S., Uehara, S., Otaka, Y., & Hirata, A. (2019). Group-level and functional-region analysis of electric-field shape during cerebellar transcranial direct current stimulation with different electrode montages. *Journal of Neural Engineering*, *16*(3), 036001.

Grossman, N., Bono, D., Dedic, N., Kodandaramaiah, S. B., Rudenko, A., Suk, H. J., Cassara, A. M., Neufeld, E., Kuster, N., Tsai, L. H., Pascual-Leone, A., & Boyden, E. S. (2017). Noninvasive deep brain stimulation via temporally interfering electric fields. *Cell*, *169*(6), 1029–1041.e16.

Guerra, A., López-Alonso, V., Cheeran, B., & Suppa, A. (2020). Variability in non-invasive brain stimulation studies: Reasons and results. *Neuroscience Letters*, *719*, 133330. https://doi.org/10.1016/j.neulet.2017.12.058

Guler, S., Dannhauer, M., Erem, B., MacLeod, R., Tucker, D., Turovets, S., Luu, P., Erdogmus, D., & Brooks, D. H. (2016). Optimization of focality and direction in dense electrode array transcranial direct current stimulation (tDCS). *Journal of Neural Engineering*, *13*(3), 1–14.

Hartwigsen, G., Bergmann, T. O., Herz, D. M., Angstmann, S., Karabanov, A., Raffin, E., Thielscher, A., & Siebner, H. R. (2015). Modeling the effects of noninvasive transcranial brain stimulation at the biophysical, network, and cognitive level. *Progress in Brain Research*, *222*, 261–287.

Héroux, M. E., Loo, C. K., Taylor, J. L., & Gandevia, S. C. (2017). Questionable science and reproducibility in electrical brain stimulation research. *PLoS One*, *12*(4), e0175635.

Horvath, J. C., Carter, O., & Forte, J. D. (2014). Transcranial direct current stimulation: Five important issues we aren't discussing (but probably should be). *Frontiers in Systems Neuroscience*, *8*, 2.

Hsu, T. Y., Juan, C. H., & Tseng, P. (2016). Individual differences and state-dependent responses in transcranial direct current stimulation. *Frontiers in Human Neuroscience*, *10*, 643.

Huang, Y., Datta, A., Bikson, M., & Parra, L. C. (2019). Realistic volumetric-approach to simulate transcranial electric stimulation—ROAST—A fully automated open-source pipeline. *Journal of Neural Engineering*, *16*(5), 056006.

Huang, Y., Liu, A. A., Lafon, B., Friedman, D., Dayan, M., Wang, X., Bikson, M., Doyle, W. K., Devinsky, O., & Parra, L. C. (2017). Measurements and models of electric fields in the in vivo human brain during transcranial electric stimulation. *eLife*, *6*, e18834.

Huang, Y., Parra, L. C., & Haufe, S. (2016). The New York head—A precise standardized volume conductor model for EEG source localization and tES targeting. *NeuroImage*, *140*, 150–162.

Hunold, A., Haueisen, J., Freitag, C. M., Siniatchkin, M., & Moliadze, V. (2021). Cortical current density magnitudes during transcranial direct current stimulation correlate with skull thickness in children, adolescent and young adults. *Progress in Brain Research*, *264*, 41–56.

Indahlastari, A., Albizu, A., Kraft, J. N., O'Shea, A., Nissim, N. R., Dunn, A. L., Carballo, D., Gordon, M. P., Taank, S., Kahn, A. T., Hernandez, C., Zucker, W. M., & Woods, A. J. (2021). Individualized tDCS modeling predicts functional connectivity changes within the working memory network in older adults. *Brain Stimulation*, *14*(5), 1205–1215. https://doi.org/10.1016/j.brs.2021.08.003

Indahlastari, A., Albizu, A., O'Shea, A., Forbes, M. A., Nissim, N. R., Kraft, J. N., Evangelista, N. D., Hausman, H. K., & Woods, A. J. (2020). Modeling transcranial electrical stimulation in the aging brain. *Brain Stimulation*, *13*(3), 664–674.

Indahlastari, A., Kasinadhuni, A. K., Saar, C., Castellano, K., Mousa, B., Chauhan, M., Mareci, T. H., & Sadleir, R. J. (2018). Methods to compare predicted and observed phosphene experience in tACS subjects. *Neural Plasticity*, *2018*, 8525706.

Jamil, A., Batsikadze, G., Kuo, H. I., Meesen, R. L. J., Dechent, P., Paulus, W., & Nitsche, M. A. (2020). Current intensity- and polarity-specific online and aftereffects of transcranial direct current stimulation: An fMRI study. *Human Brain Mapping*, *41*(6), 1644–1666.

Johnson, E. L., Arciniega, H., Jones, K. T., Kilgore-Gomez, A., & Berryhill, M. E. (2022). Individual predictors and electrophysiological signatures of working memory enhancement in aging. *NeuroImage*, *250*, 118939.

Jones, K. T., Arciniega, H., & Berryhill, M. E. (2019). Replacing tDCS with theta tACS provides selective, but not general WM benefits. *Brain Research*, *1720*, 146324.

Jones, K. T., Johnson, E. L., & Berryhill, M. E. (2020). Frontoparietal theta-gamma interactions track working memory enhancement with training and tDCS. *NeuroImage*, *211*, 116615.

Jung, Y.-J., Kim, J.-H., Kim, D., & Im, C.-H. (2013). An image-guided transcranial direct current stimulation system: A pilot phantom study. *Physiological Measurement*, *34*(8), 937–950.

Kalloch, B., Bazin, P. L., Villringer, A., Sehm, B., & Hlawitschka, M. (2020). A flexible workflow for simulating transcranial electric stimulation in healthy and lesioned brains. *PLoS One*, *15*(5), e0228119.

Karabanov, A., Thielscher, A., & Siebner, H. R. (2016). Transcranial brain stimulation: Closing the loop between brain and stimulation. *Current Opinion in Neurology*, *29*(4), 397–404.

Kasten, F. H., Duecker, K., Maack, M. C., Meiser, A., & Herrmann, C. S. (2019). Integrating electric field modeling and neuroimaging to explain inter-individual variability of tACS effects. *Nature Communications*, *10*(1), 5427.

Kessler, S. K., Minhas, P., Woods, A. J., Rosen, A., Gorman, C., & Bikson, M. (2013). Dosage considerations for transcranial direct current stimulation in children: A computational modeling study. *PLoS One*, *8*(9), e76112.

Khan, A., Antonakakis, M., Vogenauer, N., Haueisen, J., & Wolters, C. H. (2022). Individually optimized multi-channel tDCS for targeting somatosensory cortex. *Clinical Neurophysiology*, *134*, 9–26. https://doi.org/10.1016/j.clinph.2021.10.016

Kim, D., Jeong, J., Jeong, S., Kim, S., Jun, S. C., & Chung, E. (2015). Validation of computational studies for electrical brain stimulation with phantom head experiments. *Brain Stimulation*, *8*(8), 914–925.

Kim, J. H., Kim, D. W., Chang, W. H., Kim, Y. H., Kim, K., & Im, C. H. (2014). Inconsistent outcomes of transcranial direct current stimulation may originate from anatomical differences among individuals: Electric field simulation using individual MRI data. *Neuroscience Letters*, *564*, 6–10.

Klaus, J., & Schutter, D. J. L. G. (2021). Electrode montage-dependent intracranial variability in electric fields induced by cerebellar transcranial direct current stimulation. *Scientific Reports*, *11*(1), 22183.

Krause, B., & Kadosh, R. C. (2014). Not all brains are created equal: The relevance of individual differences in responsiveness to transcranial electrical stimulation. *Frontiers in Systems Neuroscience*, *8*, 25.

Kunze, T., Hunold, A., Haueisen, J., Jirsa, V., & Spiegler, A. (2016). Transcranial direct current stimulation changes resting state functional connectivity: A large-scale brain network modeling study. *NeuroImage*, *140*(October), 174–187.

Laakso, I., & Hirata, A. (2013). Computational analysis shows why transcranial alternating current stimulation induces retinal phosphenes. *Journal of Neural Engineering*, *10*(4), 046009.

Laakso, I., Mikkonen, M., Koyama, S., Hirata, A., & Tanaka, S. (2019). Can electric fields explain inter-individual variability in transcranial direct current stimulation of the motor cortex? *Scientific Reports*, *9*(1), 626.

Laakso, I., Tanaka, S., Mikkonen, M., Koyama, S., Sadato, N., & Hirata, A. (2016). Electric fields of motor and frontal tDCS in a standard brain space: A computer simulation study. *NeuroImage*, *137*, 140–151.

Lee, C., Jung, Y. J., Lee, S. J., & Im, C. H. (2017). COMETS2: An advanced MATLAB toolbox for the numerical analysis of electric fields generated by transcranial direct current stimulation. *Journal of Neuroscience Methods*, *277*, 56–62.

Lee, J. S. A., Bestmann, S., & Evans, C. (2021). A future of current flow modelling for transcranial electrical stimulation? *Current Behavioral Neuroscience Reports*, *8*, 150–159. https://doi.org/10.1007/s40473-021-00238-5

Lee, S., Lee, C., Park, J., & Im, C.-H. (2020). Individually customized transcranial temporal interference stimulation for focused modulation of deep brain structures: A simulation study with different head models. *Scientific Reports*, *10*(1), 11730.

Lefaucheur, J. P., Antal, A., Ayache, S. S., Benninger, D. H., Brunelin, J., Cogiamanian, F., Cotelli, M., De Ridder, D., Ferrucci, R., Langguth, B., Marangolo, P., Mylius, V., Nitsche, M. A., Padberg, F., Palm, U., Poulet, E., Priori, A., Rossi, S., Schecklmann, M., … Paulus, W. (2017). Evidence-based guidelines on the therapeutic use of transcranial direct current stimulation (tDCS). *Clinical Neurophysiology*, *128*(1), 56–92.

Li, L. M., Uehara, K., & Hanakawa, T. (2015). The contribution of interindividual factors to variability of response in transcranial direct current stimulation studies. *Frontiers in Cellular Neuroscience*, *9*, 181. https://doi.org/10.3389/fncel.2015.00181

Liu, A., Vöröslakos, M., Kronberg, G., Henin, S., Krause, M. R., Huang, Y., Opitz, A., Mehta, A., Pack, C. C., Krekelberg, B., Berényi, A., Parra, L. C., Melloni, L., Devinsky, O., & Buzsáki, G. (2018). Immediate neurophysiological effects of transcranial electrical stimulation. *Nature Communications*, *9*(1), 5092.

Manenti, R., Sandrini, M., Gobbi, E., Cobelli, C., Brambilla, M., Binetti, G., & Cotelli, M. (2017). Strengthening of existing episodic memories through non-invasive stimulation of prefrontal cortex in older adults with subjective memory complaints. *Frontiers in Aging Neuroscience*, *9*, 401.

Medina, J., & Cason, S. (2017). No evidential value in samples of transcranial direct current stimulation (tDCS) studies of cognition and working memory in healthy populations. *Cortex*, *94*, 131–141.

Meier, J., Nolte, G., Schneider, T. R., Engel, A. K., Leicht, G., & Mulert, C. (2019). Intrinsic 40Hz-phase asymmetries predict tACS effects during conscious auditory perception. *PLoS One*, *14*(4), e0213996.

Mendonca, M. E., Santana, M. B., Baptista, A. F., Datta, A., Bikson, M., Fregni, F., & Araujo, C. P. (2011). Transcranial DC stimulation in fibromyalgia: Optimized cortical target supported by high-resolution computational models. *Journal of Pain*, *12*(5), 610–617.

Mikkonen, M., Laakso, I., Tanaka, S., & Hirata, A. (2020). Cost of focality in TDCS: Interindividual variability in electric fields. *Brain Stimulation*, *13*(1), 117–124.

Miniussi, C., Harris, J. A., & Ruzzoli, M. (2013). Modelling non-invasive brain stimulation in cognitive neuroscience. *Neuroscience and Biobehavioral Reviews*, *37*(8), 1702–1712.

Miranda, P. C., Callejón-Leblic, M. A., Salvador, R., & Ruffini, G. (2018). Realistic modeling of transcranial current stimulation: The electric field in the brain. *Current Opinion in Biomedical Engineering*, *8*, 20–27.

Miranda, P. C., Lomarev, M., & Hallett, M. (2006). Modeling the current distribution during transcranial direct current stimulation. *Clinical Neurophysiology*, *117*(7), 1623–1629.

Mosayebi-Samani, M., Jamil, A., Salvador, R., Ruffini, G., Haueisen, J., & Nitsche, M. A. (2021). The impact of individual electrical fields and anatomical factors on the neurophysiological outcomes of tDCS: A TMS-MEP and MRI study. *Brain Stimulation*, *14*(2), 316–326.

Muffel, T., Kirsch, F., Shih, P. C., Kalloch, B., Schaumberg, S., Villringer, A., & Sehm, B. (2019). Anodal transcranial direct current stimulation over S1 differentially modulates proprioceptive accuracy in young and old adults. *Frontiers in Aging Neuroscience*, *11*, 264.

Naskovska, K., Lau, S., Korobkov, A. A., Haueisen, J., & Haardt, M. (2020). Coupled CP decomposition of simultaneous MEG-EEG signals for differentiating oscillators during photic driving. *Frontiers in Neuroscience*, *14*, 261. https://doi.org/10.3389/fnins.2020.00261

Opitz, A., Falchier, A., Yan, C. G., Yeagle, E. M., Linn, G. S., Megevand, P., Thielscher, A., Deborah, R. A., Milham, M. P., Mehta, A. D., & Schroeder, C. E. (2016). Spatiotemporal structure of intracranial electric fields induced by transcranial electric stimulation in humans and nonhuman primates. *Scientific Reports*, *6*, 31236.

Opitz, A., Paulus, W., Will, S., Antunes, A., & Thielscher, A. (2015). Determinants of the electric field during transcranial direct current stimulation. *NeuroImage*, *109*, 140–150.

Paulus, W. (2011). Transcranial electrical stimulation (tES—tDCS; tRNS, tACS) methods. *Neuropsychological Rehabilitation*, *21*(5), 602–617.

Peterchev, A. V., Wagner, T. A., Miranda, P. C., Nitsche, M. A., Paulus, W., Lisanby, S. H., Pascual-Leone, A., & Bikson, M. (2012). Fundamentals of transcranial electric and magnetic stimulation dose: Definition, selection, and reporting practices. *Brain Stimulation*, *5*(4), 435–453.

Piastra, M. C., van der Cruijsen, J., Piai, V., Jeukens, F. E. M., Manoochehri, M., Schouten, A. C., Selles, R. W., & Oostendorp, T. (2021). ASH: An automatic pipeline to generate realistic and individualized chronic stroke volume conduction head models. *Journal of Neural Engineering*, *18*(4), 044001.

Rahman, A., Reato, D., Arlotti, M., Gasca, F., Datta, A., Parra, L. C., & Bikson, M. (2013). Cellular effects of acute direct current stimulation: Somatic and synaptic terminal effects. *The Journal of Physiology*, *591*(10), 2563–2578.

Rampersad, S. M., Janssen, A. M., Lucka, F., Aydin, U., Lanfer, B., Lew, S., Wolters, C. H., Stegeman, D. F., & Oostendorp, T. F. (2014). Simulating transcranial direct current stimulation with a detailed anisotropic human head model. *IEEE Transactions on Neural Systems and Rehabilitation Engineering*, *22*(3), 441–452.

Rasmussen, I. D., Boayue, N. M., Mittner, M., Bystad, M., Grønli, O. K., Vangberg, T. R., Csifcsák, G., Aslaksen, P. M., & Peter, J. (2021). High-definition transcranial direct current stimulation improves delayed memory in Alzheimer's disease patients: A pilot study using computational modeling to optimize electrode position. *Journal of Alzheimer's Disease*, *83*(2), 753–769.

Reed, T., & Cohen Kadosh, R. (2018). Transcranial electrical stimulation (tES) mechanisms and its effects on cortical excitability and connectivity. *Journal of Inherited Metabolic Disease*, *41*(6), 1123–1130.

Reinhart, R. M. G., & Nguyen, J. A. (2019). Working memory revived in older adults by synchronizing rhythmic brain circuits. *Nature Neuroscience*, *22*(5), 820–827.

Ruffini, G., Fox, M. D., Ripolles, O., Miranda, P. C., & Pascual-Leone, A. (2014). Optimization of multifocal transcranial current stimulation for weighted cortical pattern targeting from realistic modeling of electric fields. *NeuroImage*, *89*, 216–225.

Sabel, B. A., Kresinsky, A., Cardenas-Morales, L., Haueisen, J., Hunold, A., Dannhauer, M., & Antal, A. (2021). Evaluating current density modeling of non-invasive eye and brain electrical stimulation using Phosphene thresholds. *IEEE Transactions on Neural Systems and Rehabilitation Engineering*, *29*, 2133–2141.

Sadleir, R. J., Vannorsdall, T. D., Schretlen, D. J., & Gordon, B. (2010). Transcranial direct current stimulation (tDCS) in a realistic head model. *NeuroImage*, *51*(4), 1310–1318.

Salvador, R., Biagi, M. C., Puonti, O., Splittgerber, M., Moliadze, V., Siniatchkin, M., Thielscher, A., & Ruffini, G. (2020). Personalization of multi-electrode setups in tCS/tES: Methods and advantages. In S. N. Makarov, G. M. Noetscher, & A. Nummenmaa (Eds.), *Brain and human body modeling 2020: Computational human models presented at EMBC 2019 and the BRAIN Initiative® 2019 meeting* (pp. 119–135). Springer.

Saturnino, G. B., Madsen, K. H., & Thielscher, A. (2019). Electric field simulations for transcranial brain stimulation using FEM: An efficient implementation and error analysis. *Journal of Neural Engineering*, *16*(6), 066032.

Saturnino, G. B., Thielscher, A., Madsen, K. H., Knösche, T. R., & Weise, K. (2019). A principled approach to conductivity uncertainty analysis in electric field calculations. *NeuroImage*, *188*, 821–834.

Schmidt, C., Wagner, S., Burger, M., van Rienen, U., & Wolters, C. H. (2015). Impact of uncertain head tissue conductivity in the optimization of transcranial direct current stimulation for an auditory target. *Journal of Neural Engineering*, *12*(4), 046028.

Schwab, K., Ligges, C., Jungmann, T., Hilgenfeld, B., Haueisen, J., & Witte, H. (2006). Alpha entrainment in human electroencephalogram and magnetoencephalogram recordings. *Neuroreport*, *17*(17), 1829–1833.

Soleimani, G., Saviz, M., Bikson, M., Towhidkhah, F., Kuplicki, R., Paulus, M. P., & Ekhtiari, H. (2021). Group and individual level variations between symmetric and asymmetric DLPFC montages for tDCS over large scale brain network nodes. *Scientific Reports*, *11*(1), 1271.

Splittgerber, M., Borzikowsky, C., Salvador, R., Puonti, O., Papadimitriou, K., Merschformann, C., Biagi, M. C., Stenner, T., Brauer, H., & Breitling-Ziegler, C. (2021). Multichannel anodal tDCS over the left dorsolateral prefrontal cortex in a paediatric population. *Scientific Reports*, *11*(1), 1–15.

Splittgerber, M., Salvador, R., Brauer, H., Breitling-Ziegler, C., Prehn-Kristensen, A., Krauel, K., Nowak, R., Ruffini, G., Moliadze, V., & Siniatchkin, M. (2020). Individual baseline performance and electrode montage impact on the effects of anodal tDCS over the left dorsolateral prefrontal cortex. *Frontiers in Human Neuroscience*, *14*, 349. https://doi.org/10.3389/fnhum.2020.00349

Suen, P. J. C., Doll, S., Batistuzzo, M. C., Busatto, G., Razza, L. B., Padberg, F., Mezger, E., Bulubas, L., Keeser, D., De Deng, Z., & Brunoni, A. R. (2021). Association between tDCS computational modeling and clinical outcomes in depression: Data from the ELECT-TDCS trial. *European Archives of Psychiatry and Clinical Neuroscience*, *271*(1), 101–110.

Sun, W., Dong, X., Yu, G., Shuai, L., Yuan, Y., & Ma, C. (2021). Transcranial direct current stimulation in patients after decompressive craniectomy: A finite element model to investigate factors affecting the cortical electric field. *Journal of International Medical Research*, *49*(2), 030006052094211.

Suzuki, M., Tanaka, S., Gomez-Tames, J., Okabe, T., Cho, K., Iso, N., & Hirata, A. (2022). Nonequivalent after-effects of alternating current stimulation on motor cortex oscillation and inhibition: Simulation and experimental study. *Brain Sciences*, *12*(2), 195. https://doi.org/10.3390/brainsci12020195

Tan, J., Wansbrough, K., Williams, A. G., Nitsche, M. A., Vallence, A. M., & Fujiyama, H. (2020). The importance of model-driven approaches to set stimulation intensity for multi-channel transcranial alternating current stimulation (tACS). *Brain Stimulation*, *13*(4), 1002–1004.

Thut, G., Bergmann, T. O., Fröhlich, F., Soekadar, S. R., Brittain, J.-S., Valero-Cabré, A., Sack, A. T., Miniussi, C., Antal, A., Siebner, H. R., Ziemann, U., & Herrmann, C. S. (2017). Guiding transcranial brain stimulation by EEG/MEG to interact with ongoing brain activity and associated functions: A position paper. *Clinical Neurophysiology*, *128*(5), 843–857.

Truong, D. Q., Magerowski, G., Blackburn, G. L., Bikson, M., & Alonso-Alonso, M. (2013). Computational modeling of transcranial direct current stimulation (tDCS) in obesity: Impact of head fat and dose guidelines. *NeuroImage. Clinical*, *2*, 759–766.

Tseng, P., Hsu, T. Y., Chang, C. F., Tzeng, O. J. L., Hung, D. L., Muggleton, N. G., Walsh, V., Liang, W. K., Cheng, S. K., & Juan, C. H. (2012). Unleashing potential: Transcranial direct current stimulation over the right posterior parietal cortex improves change detection in low-performing individuals. *Journal of Neuroscience*, *32*(31), 10554–10561.

Veniero, D., Benwell, C. S. Y., Ahrens, M. M., & Thut, G. (2017). Inconsistent effects of parietal α-tACS on pseudoneglect across two experiments: A failed internal replication. *Frontiers in Psychology*, *8*, 952. https://doi.org/10.3389/fpsyg.2017.00952

Vergallito, A., Feroldi, S., Pisoni, A., & Lauro, L. J. R. (2022). Inter-individual variability in tDCS effects: A narrative review on the contribution of stable, variable, and contextual factors. *Brain Sciences*, *12*(5), 522.

Vöröslakos, M., Takeuchi, Y., Brinyiczki, K., Zombori, T., Oliva, A., Fernández-Ruiz, A., Kozák, G., Kincses, Z. T., Iványi, B., Buzsáki, G., & Berényi, A. (2018). Direct effects of transcranial electric stimulation on brain circuits in rats and humans. *Nature Communications*, *9*(1), 483.

Vosskuhl, J., Strüber, D., & Herrmann, C. S. (2018). Non-invasive brain stimulation: A paradigm shift in understanding brain oscillations. *Frontiers in Human Neuroscience*, *12*, 211. https://doi.org/10.3389/fnhum.2018.00211

Wagner, S., Burger, M., & Wolters, C. H. (2016). An optimization approach for well-targeted transcranial direct current stimulation. *SIAM Journal on Applied Mathematics*, *76*(6), 2154–2174.

Wagner, S., Rampersad, S. M., Aydin, Ü., Vorwerk, J., Oostendorp, T. F., Neuling, T., Herrmann, C. S., Stegeman, D. F., & Wolters, C. H. (2014). Investigation of tDCS volume conduction effects in a highly realistic head model. *Journal of Neural Engineering*, *11*(1), 016002.

Wagner, T., Fregni, F., Fecteau, S., Grodzinsky, A., Zahn, M., & Pascual-Leone, A. (2007). Transcranial direct current stimulation: A computer-based human model study. *NeuroImage*, *35*(3), 1113–1124.

Windhoff, M., Opitz, A., & Thielscher, A. (2013). Electric field calculations in brain stimulation based on finite elements: An optimized processing pipeline for the generation and usage of accurate individual head models. *Human Brain Mapping*, *34*(4), 923–935.

Wischnewski, M., Mantell, K. E., & Opitz, A. (2021). Identifying regions in prefrontal cortex related to working memory improvement: A novel meta-analytic method using electric field modeling. *Neuroscience and Biobehavioral Reviews*, *130*, 147–161.

Zanto, T. P., Jones, K. T., Ostrand, A. E., Hsu, W. Y., Campusano, R., & Gazzaley, A. (2021). Individual differences in neuroanatomy and neurophysiology predict effects of transcranial alternating current stimulation. *Brain Stimulation*, *14*(5), 1317–1329.

How to cite this article: Hunold, A., Haueisen, J., Nees, F., & Moliadze, V. (2023). Review of individualized current flow modeling studies for transcranial electrical stimulation. *Journal of Neuroscience Research*, *101*, 405–423. https://doi.org/10.1002/jnr.25154